Shap. Mem. Superelasticity
https://doi.org/10.1007/s40830-018-0193-9

The Effect of Low Temperature Aging and the Evolution of R-Phase in Ni-Rich NiTi

Ali Shamimi[1] · Behnam Amin-Ahmadi[2] · Aaron Stebner[2] · Tom Duerig[1]

Abstract This study investigates the thermal and mechanical properties that arise from aging Ni-rich Ni–Ti (Nitinol) at temperatures below 250 °C, well below those commonly used to fabricate medical devices. We demonstrate that the $Ni_{50.8}$–$Ti_{49.2}$ composition decomposes at temperatures as low as room temperature and discuss the unusual changes in thermal and mechanical behaviors compared to common aging treatments, such as separation of Martensite and R-phase transformations. Using such aging treatments, superelasticity can be achieved without the presence of austenite at body temperature ($A_f > 45$ °C, well above the body temperature). Furthermore, the influence of R-phase on mechanical response and the disparity between thermal and mechanical behavior is discussed in detail.

Keywords Aging · R-phase · Low temperature aging · Mechanical properties · Heat treatment · NiTi < materials · Precipitation

Introduction

Aging in conjunction with cold work is widely practiced by the medical device industry to shape set, strengthen, and adjust the transformation temperatures of Ni-rich Ni–Ti alloys. These three objectives (accurately achieving the desired shape, preventing plastic deformation, and optimizing transformation temperatures) are often at odds: accurate shape setting is promoted by longer times at higher temperatures, maximizing strength requires retaining cold work and thus low temperatures and short times, and controlling transformation temperatures demands the accurate control of the heat treatment temperatures to control the volume fraction of Ni_4Ti_3 precipitation and the Ni/Ti ratio of the NiTi matrix. Commonly employed aging/shape setting temperature regimes range from 350 to 575 °C. Until recently, aging temperatures below 200 °C had been considered too low for precipitation to occur [1]. Recent studies [2], however, have shown that nickel begins to cluster at very low temperatures, eventually yielding to the coherent precipitation of Ni_4Ti_3. Similarly, a short-range atomic reordering has been reported in a high-temperature ternary system when aging at 250 °C [3].

The intent of this study is to further explore the low temperature aging of Ni-rich Ni–Ti alloys and its effect on transformation temperatures and mechanical properties. This is done both in a fully solutionized and annealed condition in which all the excess and free nickel is harbored on the NiTi lattice, and in a typical cold-worked and aged condition in which some of the nickel has already been precipitated, thus reducing the driving force for further precipitation.

These studies are of interest both to better understand the stability of shape set and aged devices, as well as to explore whether this unexplored aging regime offers interesting properties not achievable with more conventional aging regimes. To the latter point, it will be shown that these regimes allow one to independently control the stability of the two competing martensitic phases: the

✉ Ali Shamimi
ali.shamimi@nitinol.com

[1] Confluent Medical Technologies Inc., Fremont, CA, USA

[2] Colorado School of Mines, Golden, CO, USA

Published online: 18 September 2018

B19′ monoclinic Martensite[1] which we will refer to as "M," as well as the martensitic R-phase, which we will refer to as "R." Moreover, we will see that low temperature aging allows control over the hysteresis of M formation and reversion.

Before embarking, a comment on terminology is in order. The shape memory community often uses the Austenite finish temperature (A_f) as an indicator of Martensite stability and thus the plateau stresses. The fallacy of this is that it is Martensite reversion that controls the lower plateau, and in most superelastic conditions, Martensite does not revert directly to Austenite but rather to the R-phase, making A_f irrelevant to superelastic properties. Herein, we will see some rather exaggerated cases where A_f is highly misleading, including some conditions in which superelasticity is observed well below the A_f temperature. In order to avoid this confusion, we adopt a more explicit terminology [4] that specifically identifies the formation and reversion of M and R regardless of the parent phase. As is conventional, a subscripted *s*, *p*, or *f* indicates the start, peak, and finish of formation of the indicated phase (e.g., M_p indicates the temperature at which Martensite formation is most rapid). But we will superscript an asterisk to indicate the reversion of the indicated phase, e.g., M_s* indicates the start of Martensite reversion and R_f* the completion of the reversion of the R-phase. The reader can interpolate the other key temperatures from these examples.

Materials and Methods

Samples for the solutionized studies were cut from a 0.45-mm-wide and 160-μm-thick straightened binary NiTi strip with 50.8 atomic percent Nickel. Annealing was performed at 750 °C for 5 min in a furnace purged with argon, and water quenched. Aging treatments were performed as high as 200 °C and as low as 25 °C for durations of 1 h to 1 month (720 h).

The material used for cold-worked and aged studies was a superelastic binary NiTi with 50.8 atomic percent Nickel wire with 0.28-mm-diameter oxide-free surface that was cold drawn about 40%, then aged at 530 °C for 4 min to fully straighten the wire. Subsequent aging treatments were performed as high as 250 °C and as low as 25 °C for durations of 1 h to 1 month (720 h).

Differential scanning calorimetry (DSC) was performed on a TA instruments model Q100 as prescribed by the ASTM F2004 standard for Nitinol [5]. Tensile tests were performed on an Instron model 5969 equipped with an AVE2 video extensometer and in accordance with ASTM 2516 [6] with a displacement rate of 0.5 mm/min. Transmission electron microscope (TEM) characterization was performed using an FEI Talos TEM (FEG, 200 kV). The TEM samples were prepared by grinding the slices to 100–120 μm thick; a mechanical punch was then used to create 3-mm discs. A Fischione automatic twin-jet electropolisher (model 120) at 15 V was then used to thin the TEM foils. An electrolyte of 80% methanol and 20% sulphuric acid at around 5 °C was used for electropolishing.

Fig. 1 DSC measurements of $Ni_{50.8}Ti$ (at.%) samples after aging at ▶ 100 °C, 150 °C, and 200 °C for various times. The traces on the left indicate the forward exothermic direction (cooling) and those on the right the reverse endothermic direction (heating). DSC traces showing suppression of Martensite after aging the solution treated condition at 100 °C, 150 °C, and 200 °C

Results

The Solution Treated and Quenched Condition

Figure 1 shows the forward and reverse transformation temperatures after aging the fully solutionized $Ni_{50.8}Ti$ (at.%) samples at 100 °C, 150 °C, and 200 °C for various times. The dashed line at the bottom of each plot represents the unaged baseline condition. The peak transformations are labeled as the formation of Martensite (M_p) and the reversion of Martensite (M_p*). In the fully solutionized case, the parent phase in both directions is Austenite—no R-phase is evident. Figure 1 also highlights the suppression of Martensite in both forward and reverse directions. Suppression of the reverse transformation is also more marked than the forward, indicating an increase in hysteresis.

As discussed earlier, aging depletes the NiTi compound of nickel, stabilizing Martensite. Yet here we see the opposite effect: the depression of transformation temperatures to and from Martensite—a stabilization of the parent phase. But in addition to these compositional or chemical influences there are several effects related to local lattice distortions and interfacial pinning. These will be discussed later, but evidently, during low temperature aging these factors overwhelm the compositional effects and suppress Martensite.

Transmission electron microscopy (TEM) was performed to compare the microstructure of the $Ni_{50.8}Ti$ (at.%) sample after solution treatment (Fig. 2) with the sample after aging at 100 °C for 105 h (Fig. 3). Both the selected area electron diffraction (SAED) pattern and the high-

[1] Recognizing that the R-phase is a martensitic transformation, the use of the capitalized term "Martensite" will refer exclusively to the B19′ martensitic phase.

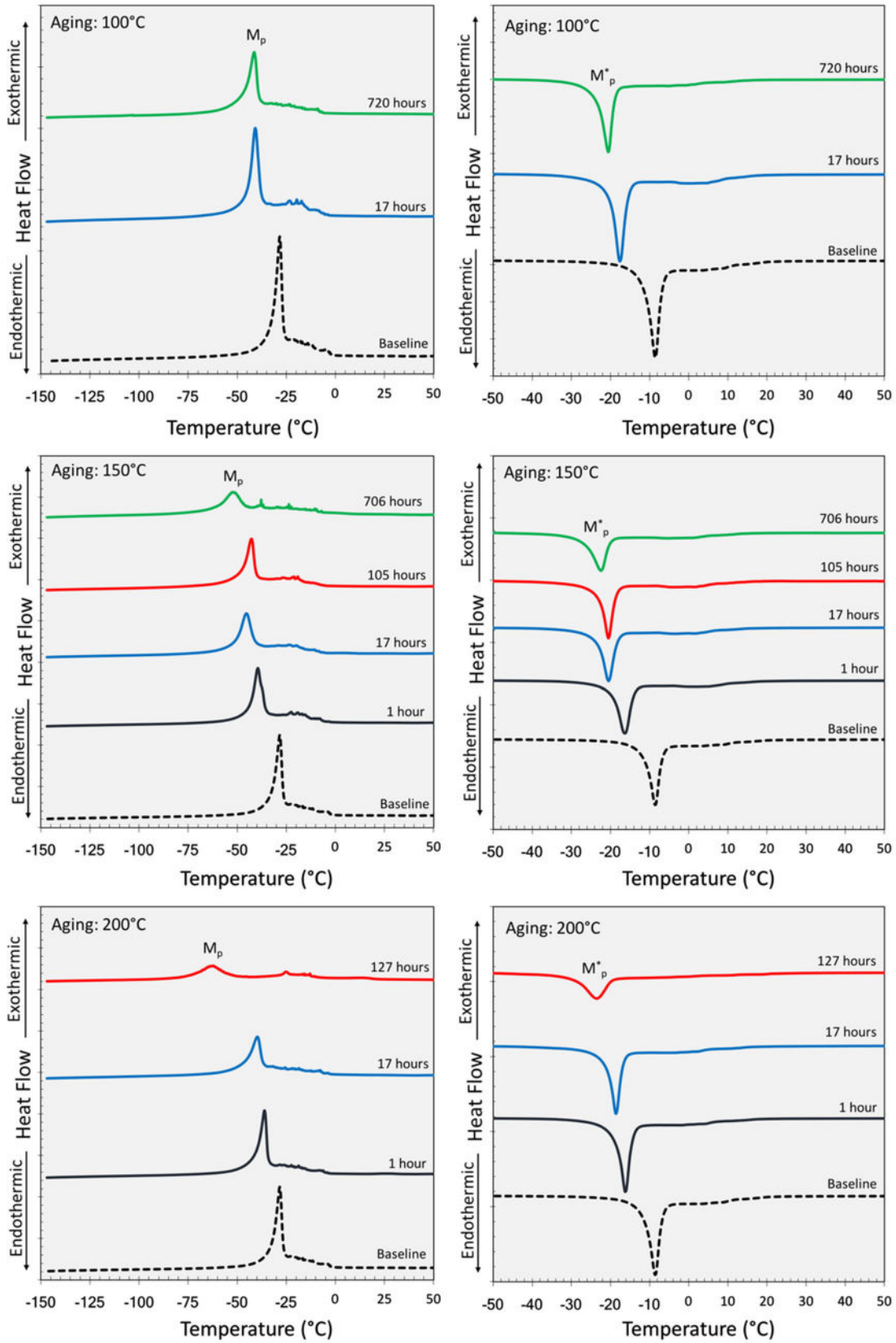
Aging: 100°C
M_p
720 hours
17 hours
Baseline
Exothermic
Heat Flow
Endothermic
-150 -125 -100 -75 -50 -25 0 25 50
Temperature (°C)
Aging: 100°C
M^*_p
720 hours
17 hours
Baseline
Exothermic
Heat Flow
Endothermic
-50 -40 -30 -20 -10 0 10 20 30 40 50
Temperature (°C)
Aging: 150°C
M_p
706 hours
105 hours
17 hours
1 hour
Baseline
Exothermic
Heat Flow
Endothermic
-150 -125 -100 -75 -50 -25 0 25 50
Temperature (°C)
Aging: 150°C
M^*_p
706 hours
105 hours
17 hours
1 hour
Baseline
Exothermic
Heat Flow
Endothermic
-50 -40 -30 -20 -10 0 10 20 30 40 50
Temperature (°C)
Aging: 200°C
M_p
127 hours
17 hours
1 hour
Baseline
Exothermic
Heat Flow
Endothermic
-150 -125 -100 -75 -50 -25 0 25 50
Temperature (°C)
Aging: 200°C
M^*_p
127 hours
17 hours
1 hour
Baseline
Exothermic
Heat Flow
Endothermic
-50 -40 -30 -20 -10 0 10 20 30 40 50
Temperature (°C)

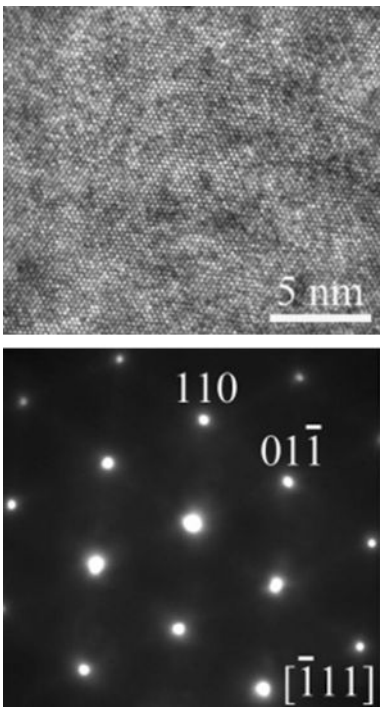

Fig. 2 High-resolution TEM image (top) and associated diffraction pattern (bottom) of unaged sample after only solution treatment (750 °C for 5 min) of $Ni_{50.8}Ti$ (at.%) showing the presence of B2 structure with no evidence of Ni_4Ti_3 precipitation

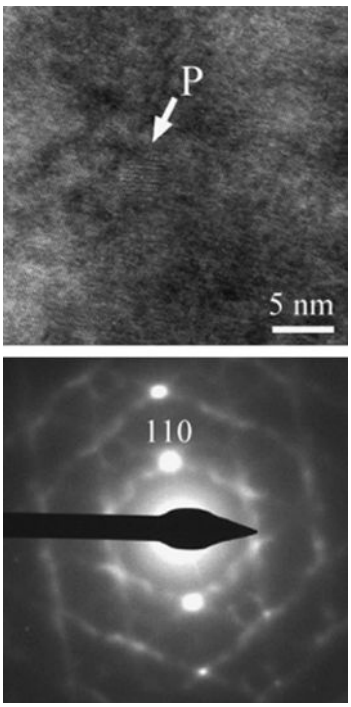

Fig. 3 High-resolution TEM image (top) and associated diffraction pattern (bottom) of $Ni_{50.8}Ti$ (at.%) sample aged at 100 °C for 105 h showing evidence of precipitation. The diffraction pattern also shows diffused intensities evident of Ni clustering

resolution TEM (HRTEM) image of the solutionized condition confirm the existence of B2 austenite structure with no evidence of precipitation. In contrast, the aged sample (Fig. 3) revealed the presence of few nano-Ni_4Ti_3 precipitates on the order of 5 nm. Also, the SAED pattern showed diffused intensities when the sample was tilted along the [110] direction, suggesting evidence of nickel clustering. This observation is consistent with what other researchers have reported [2]. The existence of such clusters of pure Ni atoms along $< 111 >_{B2}$ directions is believed to be a precursor to actual Ni_4Ti_3 precipitation [2]. Zheng et al. ascribed a suppression of the B2 to B19′ Martensitic transformation to such atomic rearrangement [7]. They hypothesized that such atomic shuffling, possibly GP zones, affects the level of ordering of the B2 matrix, causing the decrease in temperature and latent heat of the martensitic transformation.

The Cold-Worked and Aged Condition

Figure 4 shows the effect of low temperature aging at 100 °C, 150 °C, 200 °C, and 250 °C for 1 h up to 720 h on cold-worked $Ni_{50.8}Ti$ (at.%) sample which was initially aged at 530 °C for 4.5 min. This condition (cold worked and aged) typifies the processing and properties of most superelastic medical devices. The most notable difference between these curves and the solutionized DSC traces (Fig. 1) is the presence of the R-phase transformation in both the forward and reverse transformation directions. The R-phase has replaced Austenite as the parent phase of Martensite, clarifying why it is misleading to use the term A_f when one is interested in the thermodynamics of Martensite reversion. Again, clear aging effects are observed at temperatures as low as 100 °C. This is somewhat surprising since the starting condition has already been aged at 530 °C (the "baseline" condition). So, while some Ni_4Ti_3 is present prior to the additional low temperature aging, there remains a sufficient driving force for additional precipitation.

Similar to the solution-treated samples, initial aging shows clear suppression of both Martensite formation (M_p) and reversion (M_p*), though this trend is reversed at the longer times and higher aging temperatures. It should be noted that the strength of the peak associated with Martensite formation appears to weaken as Martensite is suppressed (see, for example, the scan after aging 720 h at 200 °C). This is presumably due to a combination of a weakening ΔH and a declining sensitivity in the DSC itself, though it has been argued that it may also be caused by a strain-driven transition to a glassy state [8]. We also observe that R-phase formation and reversion are not suppressed by aging and in fact appear to be stabilized (the

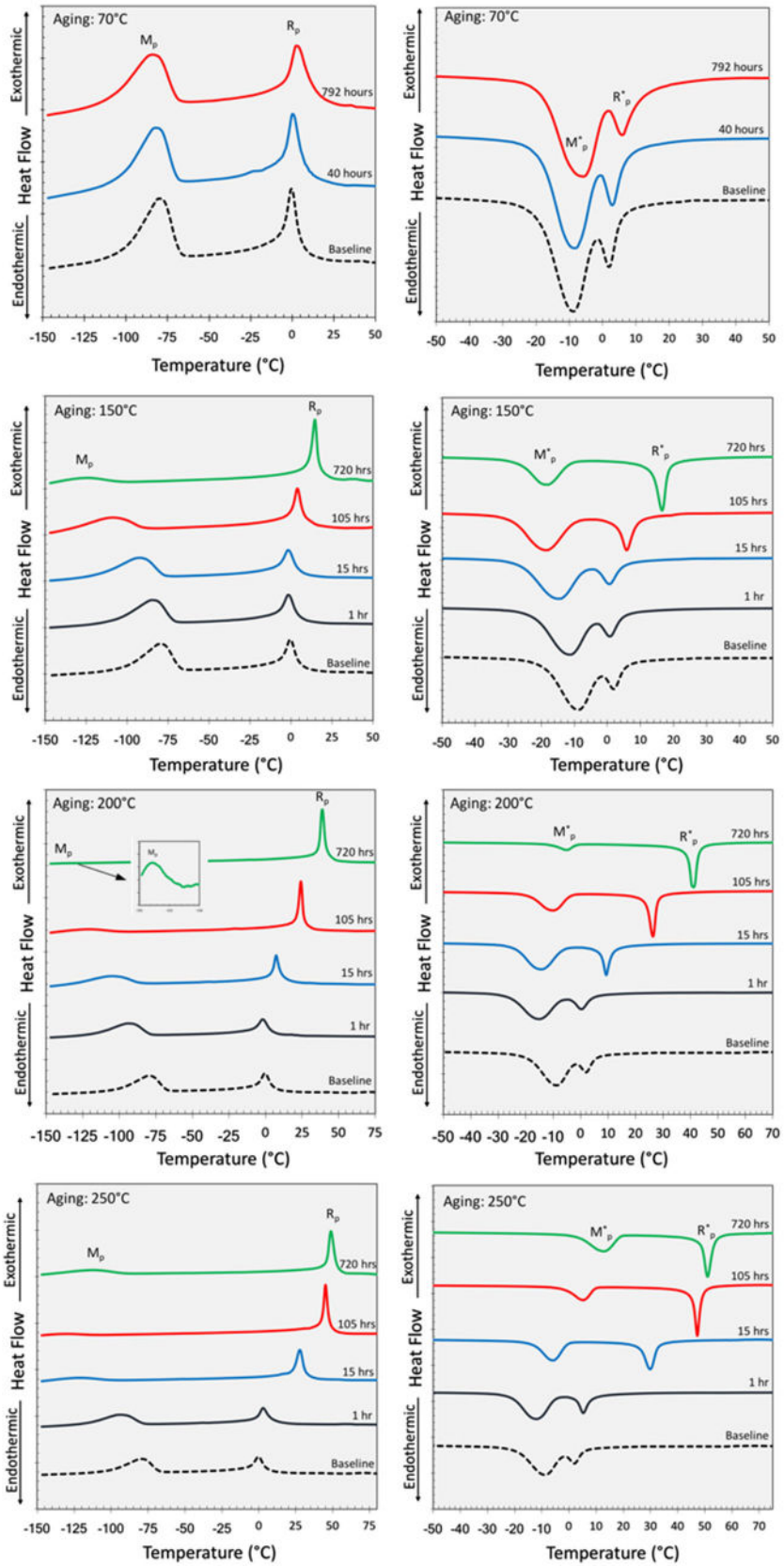

Fig. 4 DSC graphs showing forward (left) and reverse (right) transformations of $Ni_{50.8}Ti$ (at.%) after aging at 70 °C, 100 °C, 150 °C, 200 °C, and 250 °C for various times. The inset in the 200 °C curve shows more sensitive heat flow in order to identify M_p

R-phase formation (R_p) and reversion (R_p*) peaks are moved upward).

Figure 5 shows tensile curves for all cold-worked and aged conditions that were further aged at low temperatures. At 100 °C and 150 °C, a slight increase in plateau stresses is observed with exposure time, consistent with the suppression of Martensite transformation observed in DSC scans. Also, no changes in the ultimate tensile strength are observed at these lower aging temperatures, suggesting that the mechanism causing Martensite suppression does not produce significant strengthening.

Aging at 200 °C and 250 °C produces an initial increase in plateau height followed by a decrease at longer aging times. The initial increase is consistent with suppression of both Martensite formation and reversion temperatures, however the loss of stiffness at longer times appears to be inconsistent with the continued Martensite suppression indicated in the DSC results. In other words, transformation temperatures are declining, and so are the plateau heights, particularly the unloading plateau. This seeming contradiction will be explained in the next section.

Discussion

Aging, whether resulting in nickel clustering or the precipitation of Ni_4Ti_3, Ni_3Ti_2 or Ni_2Ti, enriches the NiTi matrix in titanium which in turn stabilizes B19′ Martensite.

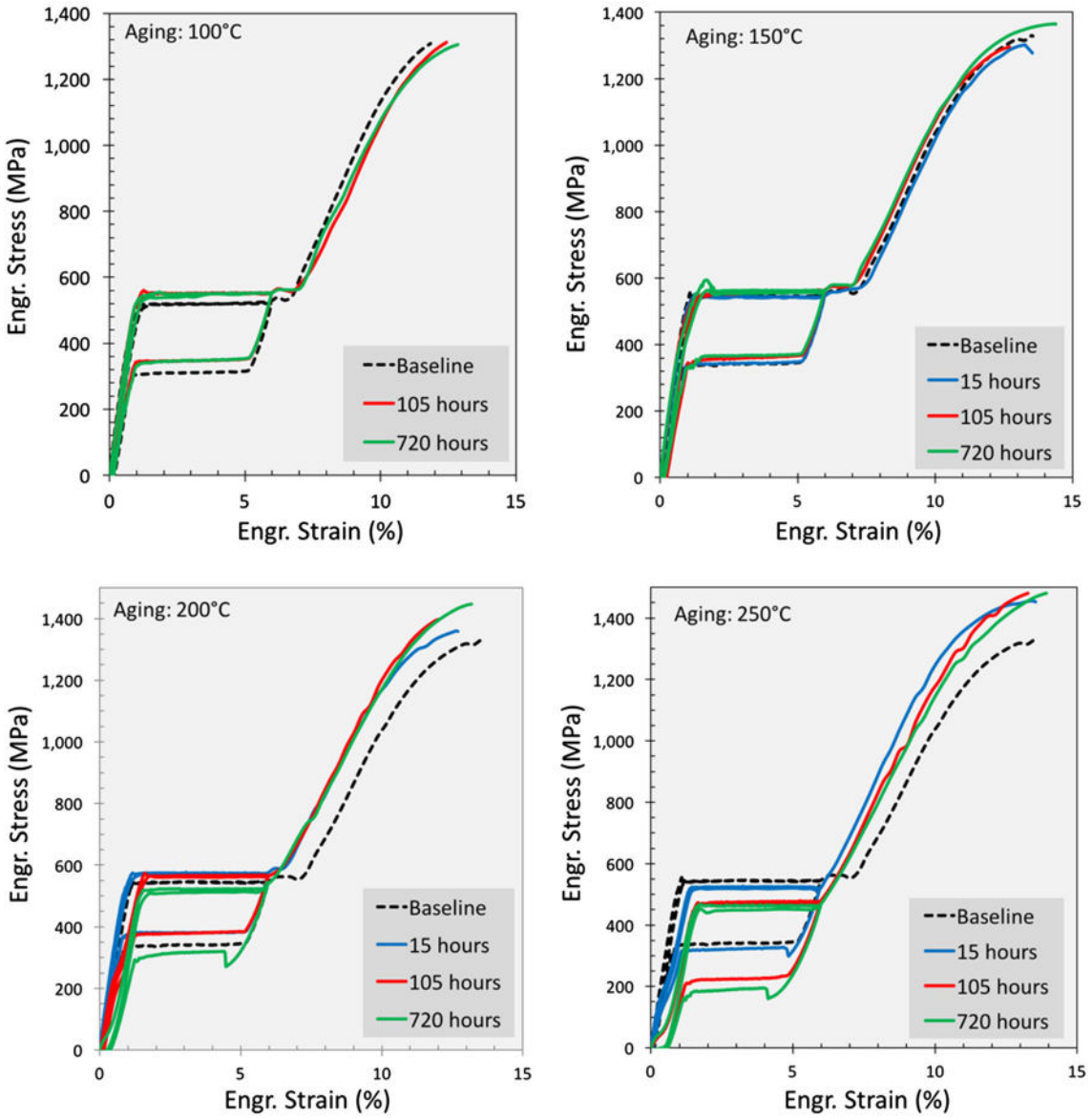

Fig. 5 Tensile test results at 37 °C after aging at 100 °C, 150 °C, 200 °C, and 250 °C. Samples were deformed to 6%, unloaded, and then pulled to fracture

Yet aging at very low temperatures results in the opposite trend: a suppression of Martensite. This was shown in the solution-treated case in which the parent phase is Austenite, as well as a cold-worked and aged condition in which the parent phase is the R-phase. But there are several contributions to stability other than the matrix chemistry that need to be considered. For example, both nickel substitutional defects and precipitates give rise to localized lattice distortions and associated elastic stress fields that affect the relative stabilities of Austenite, Martensite, and the R-phase. In the unaged condition, substitutional defects have been argued to locally stabilize an R-phase-like order [9]. During aging, whether resulting in clustering or precipitation, the population of these point defects is reduced in favor of three-dimensional precipitates producing strain fields that are anisotropic in nature. One would expect these anisotropic fields to stabilize the B19′ phase. But again, this is the opposite of what is observed.

However, one needs to also consider the kinetics of interface motion. Microstructural inhomogeneities should be expected to act as pinning sites, impeding interface mobility and thus suppressing the progress of the Martensite transformation, consistent with the observations reported above. Ultimately, as precipitate coherency is lost and the intensity of the stress inhomogeneities is reduced, the effects of matrix composition dominate and transformation temperatures rise.

These same effects might be expected to apply to the R-phase with respect to its parent, Austenite. But because of the low $\Delta\varepsilon$ associated with the R-phase, one expects a reduced interaction with stress fields. The sharp increase in R and R^* temperatures indicates that the R-phase too is stabilized by the titanium enrichment that occurs during the aging process. Lacking a significant elastic energy pinning effect, there is an immediate rise in R and R^*, which results in the observed dramatic separation between R and M transformations.

To illustrate the impact of these low temperature aging regimes, Fig. 6 compares three conditions drawn from the above set of data, representing the following three conditions:

A-to-M upon loading and M-to-A upon unloading (dashed unaged curve),
A-to-R-to-M upon loading and M-to-R upon unloading (blue curve), and

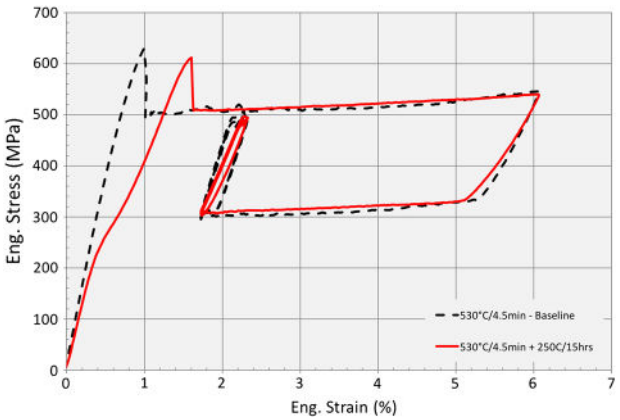

Fig. 7 Duty cycle comparison of A-M versus R-M superelasticity at 37 °C showing the difference in the duty cycle modulus after unloading and constraining on the lower plateau

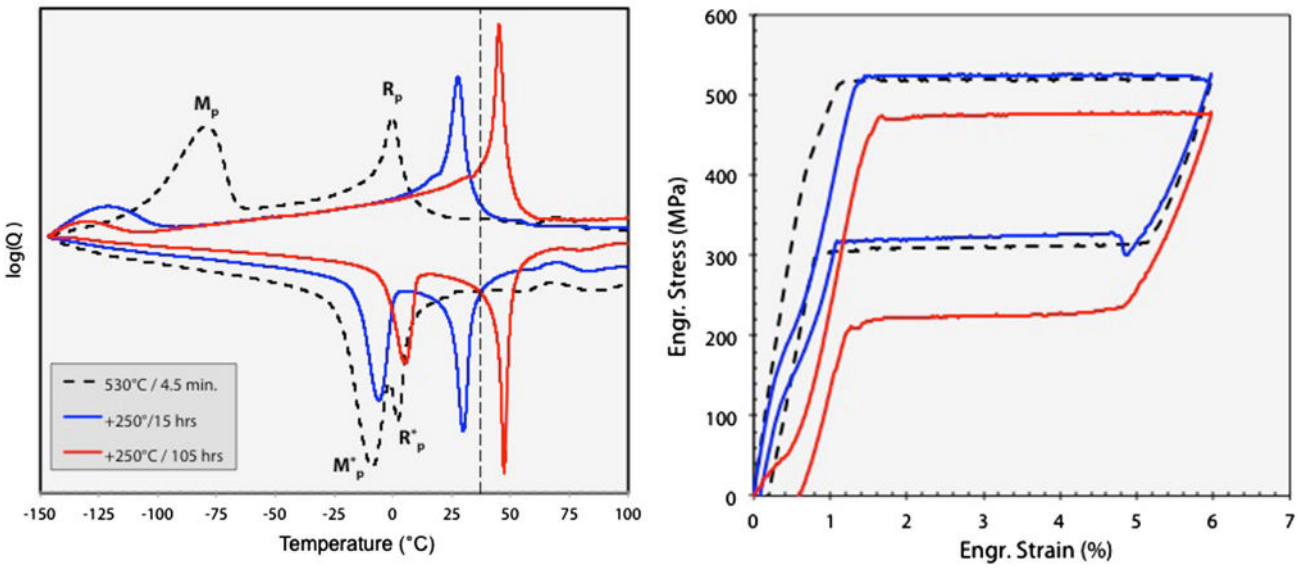

Fig. 6 Shown are the DSC and 37 °C tensile curves of the same wire heat treated three different ways, highlighting that plateaus are not dependent upon A_f. The vertical-dashed line indicates body temperature

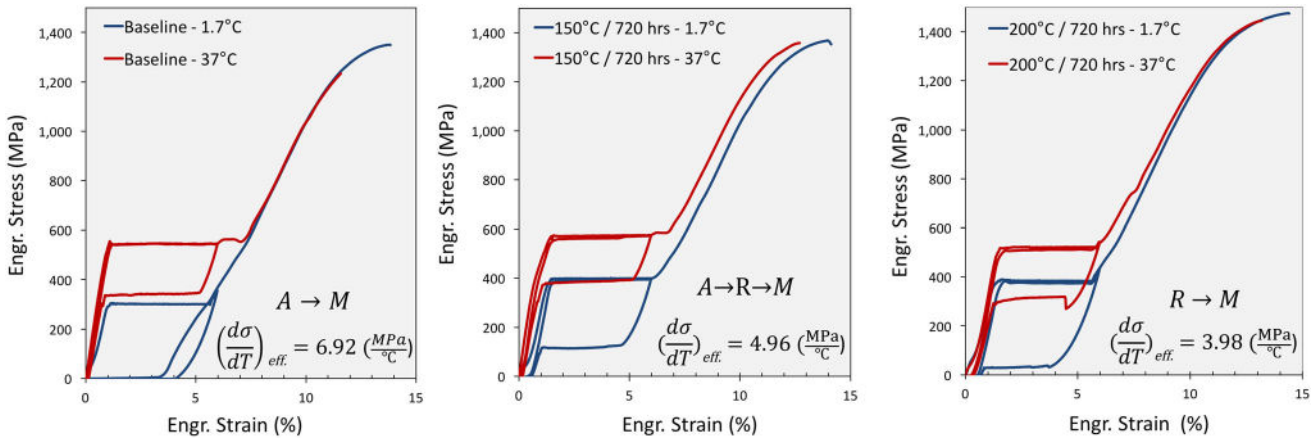

Fig. 8 Changes in the loading ($d\sigma/dT_{eff}$) with aging and R-phase stabilization are highlighted in the stress strain curves determined at 2 °C (blue) and 37 °C (red). Also note the marked reverse yield drop in the 37 °C test after aging at 200 °C for 720 h

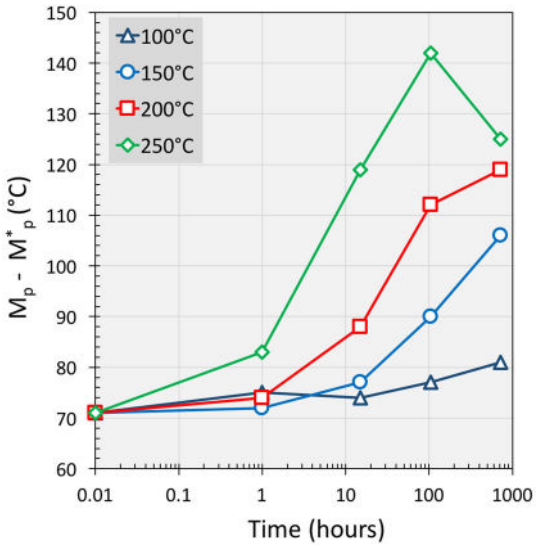

Fig. 9 Evolution of hysteresis with aging temperature and time

R-to-M upon loading and M-to-R upon unloading (red curve)

The first of these, with no additional aging, represents the typical superelastic behavior used in medical devices. The last scenario (aged 105 h at 250 °C) is perhaps the most intriguing in that we have quite satisfactory superelasticity at body temperature without the presence of Austenite (A_f is greater than 37 °C). It remains unclear just what the practical advantages or disadvantages are of such a condition. One could argue that the superelasticity is imperfect since unloading returns a twinned R-phase and thus a set of as much as 0.5%. But this can easily be taken into account in the design of a product and thus would rarely be a limitation. More to the point is that the length of the plateau is shortened by as much as 0.5% ($\Delta\varepsilon_{M\text{-}R}$ is less than $\Delta\varepsilon_{M\text{-}A}$). This may be relevant to some products, though that seems unlikely. Most noteworthy is that when a device is constrained on the unloading plateau, there is a mixture of R and M rather than a mixture of A and M. This provides a lower modulus and greater ability to elastically accommodate a duty cycle without advancing Martensite interfaces. This, in turn, should lead to a more fatigue durable structure (see Fig. 7), but this requires further exploration.

Figure 6 also highlights certain seeming discrepancies between the DSC traces and tensile properties. This is also seen in Fig. 5 showing a suppression of the thermal formation and reversion of Martensite, yet lower loading and unloading plateaus—aging for 105 h at 250 °C makes it more difficult to thermally induce Martensite, yet easier to stress induce Martensite. These observations appear at first glance to be incongruous, but such is not the case. Plateau stresses are determined by $d\sigma/dT$ times the difference between ambient temperature and the relevant transformation temperature. For example, the beginning of the loading plateau is determined by

$$\sigma_{\text{loading,start}} = (T - M_s)\, d\sigma/dT = (T - M_s)\,(-\Delta S/\Delta\varepsilon) \quad (1)$$

But in all these conditions, there are three transformations and therefore three Clausius-Clapeyron coefficients: $(d\sigma/dT)_{A\text{-}R}$, $(d\sigma/dT)_{A\text{-}M}$, and $(d\sigma/dT)_{R\text{-}M}$. And where these three trajectories intersect on a stress-temperature phase diagram, there is a triple point, hence using the term "effective" Clausius-Clapeyron coefficient, or $(d\sigma/dT)_{eff}$. In alloy systems where there is no R-phase, $(d\sigma/dT)_{eff} = (d\sigma/dT)_{A\text{-}M}$ which is typically about 6–7 MPa/°C.[2] In contrast, in materials with a A/R/M triple point above ambient

[2] This range is typical for wire or tubing measured in tension. Values depend on deformation mode and crystallographic texture.

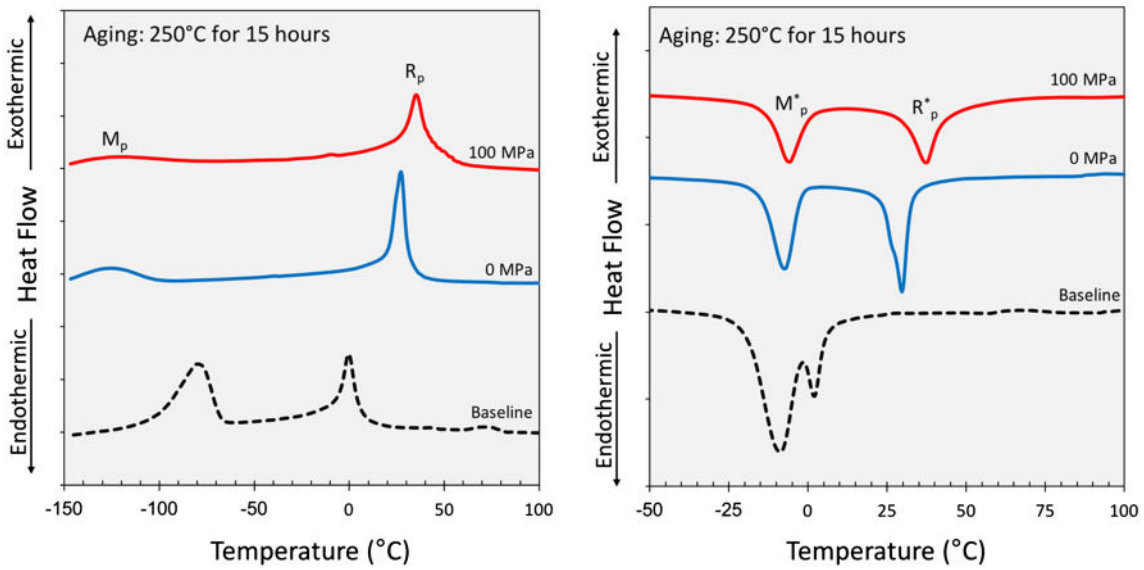

Fig. 10 DSC graphs showing forward (left) and reverse (right) transformations after aging at 250 °C for 15 h, with and without applied stress. Dashed line is the baseline sample before the low temperature aging

temperature, $(d\sigma/dT)_{eff} = (d\sigma/dT)_{R\text{-}M}$ which is typically 3.5–4.0 MPa/°C.

The most common case is when the triple point lies between M_p and ambient temperature, in which case $(d\sigma/dT)_{eff}$ is a weighted average of $(d\sigma/dT)_{A\text{-}M}$, and $(d\sigma/dT)_{R\text{-}M}$. More detail on this construction can be found in Ref. [4], but suffice it to say that as the R-phase is stabilized, the triple point increases in temperature, and $(d\sigma/dT)_{eff}$ sharply decreases. Comparing the blue and dashed conditions in Fig. 6, we see that aging at 250 °C sharply suppresses Martensite, but because the R-phase is stabilized, the stress strain curves are essentially unchanged—the increased interval between ambient temperature and the transformation temperatures are offset by the decreased $(d\sigma/dT)_{eff}$. To verify this, Fig. 8 shows the $(d\sigma/dT)_{eff}$ for the three exemplary cases, and indeed we observe a marked decrease in $(d\sigma/dT)_{eff}$ as R is stabilized.

Finally, there are kinetic factors contributing the relationship between plateau stresses and transformation temperatures. Strain localization, or Lüders deformation [10, 11], is a well-known yet often ignored phenomenon in superelastic conditions exposed to uniaxial tension. In short, when the elastic influences of individual Martensite pockets impinge, they can reduce the total strain energy by coalescing into bands spanning the entire cross section. This not only reduces the total interfacial area, it allows the volume fraction of Martensite to grow without further increases in strain energy. One often observes a drop in stress when the bands are formed, and then once formed, the plateaus are "perfectly" flat. In these cases, it is the M_s temperature that is best associated with the plateau height. The same is observed when Martensite retreats, with a reverse yield drop and a flat unloading plateau.

The relevance of the above to what is observed here is exemplified by the longest of the aged conditions at 200 °C and 250 °C. Here we begin to see a more pronounced reverse yield drop upon unloading, indicating that a great deal of strain energy is being relieved by the formation of bands. Since strain localization only occurs in the presence of tensile stresses, the same strain energy savings is not observed in a stress-free DSC test, so we expect unloading plateaus to be higher than those predicted by DSC. Thus, as the thermal hysteresis increases as shown in Fig. 9, we expect greater energy savings through the formation of Lüders bands, and consequently higher unloading plateaus.

Conclusions

It has been shown that Ni-rich Ti–Ni alloys are metastable even at temperatures as low as 100 °C, both in the solution treated and quenched condition and in the cold-worked and aged conditions typically used by the medical device industry. While the suppression in Martensite transformation temperatures and plateau stresses are not pronounced below 200 °C, many medical devices specify transformation temperature ranges as tight as ± 3 °C. Moreover, these temperatures are not uncommon in a host of processing operations such as co-extrusion and the application and curing of various coatings.

In addition to the suppression of Martensite, one observes a stabilization of the R-phase. This means the

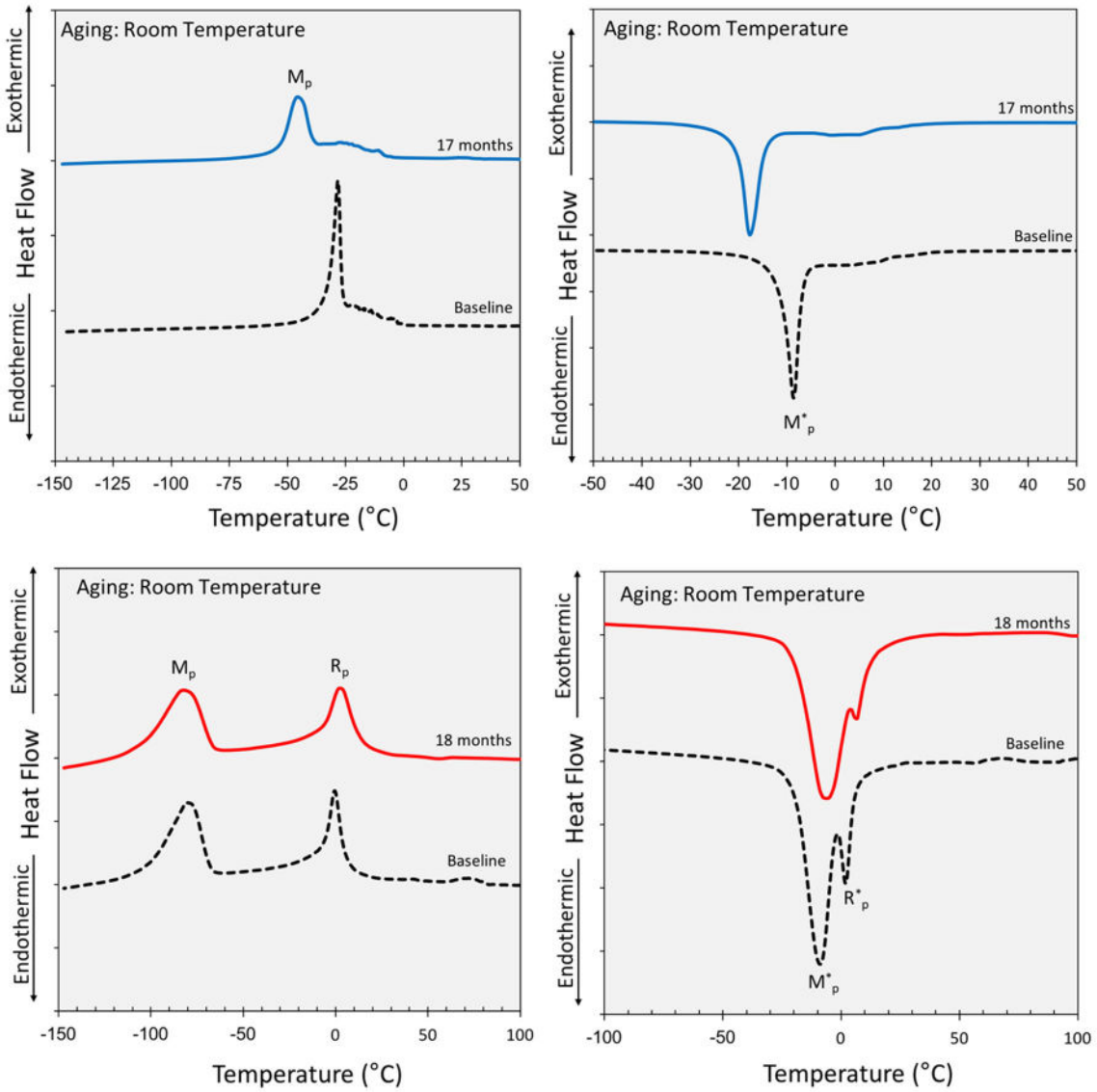

Fig. 11 DSC graphs showing the effect of aging at room temperature after 18 months of shelf life. Top is solution treated and bottom is cold-worked and aged condition. Left graphs exhibit the forward and the right graphs are the reverse transformations

R_f* (or A_f) temperature can be increased even while Martensite reversion is suppressed and the unloading plateau lifted. The increased separation of the R and M transformations allows one to establish robust superelasticity at body temperature between the R and M phases, without the appearance of Austenite ($A_f > 37$ °C). This, in turn, leads to a more compliant duty cycle with greater elastic range, and potentially greater displacement controlled durability.

These studies also point out the need for further work. For example, the trends shown in this study are accelerated by the presence of a stress, an example of which is shown in Fig. 10. Similar trends of aging under stress have been reported by other researchers [9] but further study at these very low temperatures is needed.

Very limited data also indicate that decomposition occurs at much lower temperatures than those studies here. For example, Fig. 11 specifies that in the solution treated and quenched condition, some decomposition even occurs at room temperature. This room temperature aging is consistent with other researchers' findings [12, 13]. Again, more detailed studies are in order, particularly if stress indeed accelerates these shifts. This would indicate that the stress applied by a statically constrained device might shift, potentially up or down with time, with possible implications to shelf life.

References

1. Kim JI, Miyazaki S (2005) Effect of nano-scaled precipitates on shape memory behavior of Ti-50.9 at.% Ni alloy. Acta Mater 53:4545–4554
2. Pourbabak S, Wang X, Van Dyck D, Verlinden B, Schryvers D (2017) Ni cluster formation in low temperature annealed $Ni_{50.6}$-$Ti_{49.4}$. Funct Mater Lett 10(1):1740005
3. Pérez-Sierra AM, Pons J, Santamarta R, Karaman I, Noebe RD (2016) Stability of a Ni-rich Ni-Ti-Zr high temperature shape memory alloy upon low temperature aging and thermal cycling. Scr Mater 124:47–50
4. Duerig TW, Pelton AR, Bhattacharya K (2017) The measurement and interpretation of transformation temperatures in Nitinol. Shape Mem Superelast 3:485–498
5. ASTM Designation: F 2004–16 (2000) Standard test method for transformation temperature of nickel–titanium alloys by thermal analysis
6. ASTM Designation: F 2516–14 (2006) Standard test method for tension testing of nickel–titanium superelastic materials
7. Zheng Y, Jiang F, Li L, Yang H, Liu Y (2008) Effect of ageing treatment on the transformation behaviour of Ti–50.9 at.% Ni alloy. Acta Mater 56:736–745
8. Zhou Z, Cui J, Ren X (2015) Strain glass state as the boundary of two phase transitions. Sci Rep 5:13377
9. Khalil-Allafi J, Dlouhy A, Eggeler G (2002) Ni_4Ti_3-precipitation during aging of NiTi shape memory alloys and its influence on martensitic phase transformations. Acta Mater 50:4255–4274
10. Reedlunn B, Churchill CB, Nelson EE, Shaw JA, Daly SH (2014) Tension, compression, and bending of superelastic shape memory alloy tubes. J Mech Phys Solids 63:506–537
11. Feng P, Sun QP (2006) Experimental investigation on macroscopic domain formation and evolution in polycrystalline NiTi microtubing under mechanical force. J Mech Phys Solids 54:1568–1603
12. Kustov S, Mas B, Salas D, Cesari E, Raufov S, Nikolaev V, Van Humbeeck J (2015) On the effect of room temperature ageing of Ni-rich Ni–Ti alloys. Scr Mater 103:10–13
13. Kustov S, Mas B, Kuskarbaev Z, Wang X, Van Humbeeck J (2016) Reply to comment on: on the effect of room temperature ageing of Ni-rich Ni–Ti alloys. Scr Mater 123:166–168